Application of seismic methods for geotechnical site characterization

P.M. Soupios
Technological Educational Institute of Crete, Department of Natural Resources & Environment, Laboratory of Geophysics & Seismology, Hania, Greece

C.B. Papazachos, G. Vargemezis and I. Fikos
Geophysical Laboratory, Aristotle University of Thessaloniki, Macedonia, Greece

ABSTRACT

There is an increasing requirement for geophysical surveys carried out during geotechnical investigations to provide direct information about rock quality or other geotechnical parameters. With the paucity of information to correlate geophysical results with actual rock properties, this is still difficult to achieve and additional research effort needs to be performed to address this issue. Nowadays, several researchers have been described detailed studies which designed specifically to investigate this matter.

Generally, geophysical techniques which are used to estimate seismic velocities in the subsurface focus on the low strain levels that are not large enough to induce significant nonlinear, nonelastic stress-strain behavior (Luna and Jadi, 2000), which is normally evaluated when addressing liquefaction potential of soils in the shallow subsurface. Soil parameters relevant to seismic ground response (Rechtien, 1996) are density, relative density and void ratio, permeability, shear modulus, water saturation, soil fabric and stress history. Detailed characterization of elastic properties near a major construction site (e.g. a bridge) is useful for near field dynamic analysis of soil-structure interaction (SSI) effects. The coupled effect of the bridge foundation (piles, piers or abutments) and the soil immediately surrounding these substructure elements is essential for dynamic SSI analysis of these critical bridge structures.

This paper presents a geophysical investigation performed along the under construction highway of Egnatia Odos, approximately 13 km west from the town of Xanthi in N. Greece. Twelve geotechnical boreholes, drilled at the maximum depth of 75 m, approximately located 20 m from the Nestos River. The objective of the survey was to obtain the high-resolution compressional and shear wave velocities of the shallow subsurface for computation of elastic engineering properties of the unconsolidated material interposed between the investigated boreholes. Joint interpretation of borehole logs and velocity images obtained by P- and S-wave traveltime inversions outlined shallow geological anomalies.

1. INTRODUCTION

The seismic method is a powerful geophysical exploration technique that has been in widespread use in ground engineering for more than 40 years and has been increasingly used since 1996 in geotechnical and environmental applications, usually at depths shallower than 40 meters. The applicability of seismic methods depends on the presence of acoustical contrasts in the subsurface. In many cases the acoustical contrasts occur at boundaries between geological layers, although man-made boundaries such as tunnels and mines also present contrasts.

Seismic survey is the geophysical method, which is most closely related to rock and soil mass properties, since seismic wave velocity varies with the main mechanical properties, such as Poisson's ratios and others modules. The earliest applications of the method primarily concerned the determination of the depth to bedrock beneath a soil cover. Later, the same method was used successfully for the location of "weak" zones, such as shear zones and faults. Nowadays, seismic methods have been used in connection with planning of dams (e.g. Klimis

et al., 1999), tunnels and portals.

The field measurements can be carried out on the surface, in boreholes, or even on the seabed. The necessity of a borehole controls the overall geophysical cost which is increased unless boring is also needed for other geotechnical purposes (CPT/SPT tests, etc). Recently, most scientists prefer to apply Crosshole and Downhole Seismics (CHS and DHS) tests, since it is highly accurate method for determining material properties of rock and soil sites. Thin low-velocity layers lying between high velocity layers can be detected with this method, which may not be possible with surface methods. In addition, the accuracy and resolution of the CHS and DHS methods is almost constant for all test depths, whereas the accuracy and resolution of the surface methods decreases with depth. A limitation of these methods is to generate adequate energy without damaging the borehole casing.

The present work is a link in a series of activities aiming at implementing geophysical methods for geotechnical engineering. Specifically, CHS and DHS measurements are performed in five selected places in the area of Nestos river in order to obtain information on dynamic soil and rock properties for earthquake design analyses for bridge construction. Tests determine shear and compression wave velocity profiles versus depth and other crucial parameters such as Poisson’s ratios, Young and Rigidity modules. Complementary, the attenuation model for two areas (where three boreholes are used) were also calculated applying spectral-ratio technique to waveforms, as suggested by Sams and Goldberg (1990) and Neep et al., (1996).

2. STUDY AREA & DATA ACQUISITION

The investigation area is located in the eastern part of Greece, thirteen kilometers from the town of Xanthi. The main geological formations of the area are shown in Figure 1. The general geology of the area consists of gravels, coarse sand, moraine (20+ meter thick) overlying semi-consolidated pleistocenic sediments consisting of cemented gravel and sand, occasionally with big blocks of limestones. The basement consists of fractured gneiss, gneiss schist and mica schist. Sedimentary layers become thicker and more cohesive with depth. The free ground water level is normally located 3.4 meters below

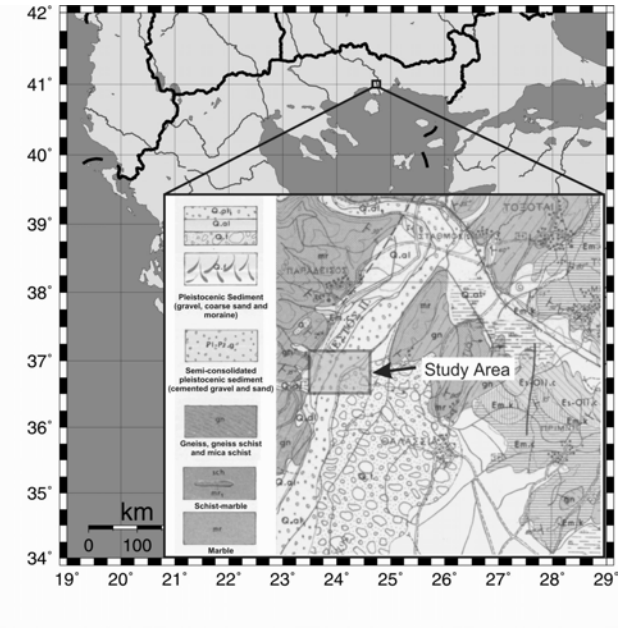

Figure 1: Map of Greece showing the area of the foundation of Nestos Bridge. A geological map of the site with the main formations is also presented.

the ground surface (due to the adjacent Nestos river) and the pore water pressure is hydrostatic from this level.

For seismic tests 12 boreholes were constructed using a water drilling machine. The borehole setup is shown in Figure 2.

In CH1 and CH3, three boreholes are used in order to also obtain an estimation of the attenuation model with depth. The boreholes were 4.5 inches in diameter, PVC cased and grouted according the American Standards (ASTM D4428/D4428M-84) to ensure good transmission of the wave energy. The hole must usually be cased and grouted to prevent the soil from caving in during the testing. The distances between adjacent boreholes were of the order of 3.5 meters.

The source and receiver boreholes are drilled to the total depth of investigation. The source is lowered to the measurements depth and one or two receivers were lowered to the same depth in the others boreholes. To generate shear and compression wave energy, we used the BGS Cross hole shear-wave electromagnetic hammer with inflated tube clamping system. To record the generated pulse we used two similar tri-axial GEOSTUFF geophones (BHG-2 model) clamped to the borehole wall by means of a motor-driven bow-springs. The vertical component of the receiver is used to capture the vertically

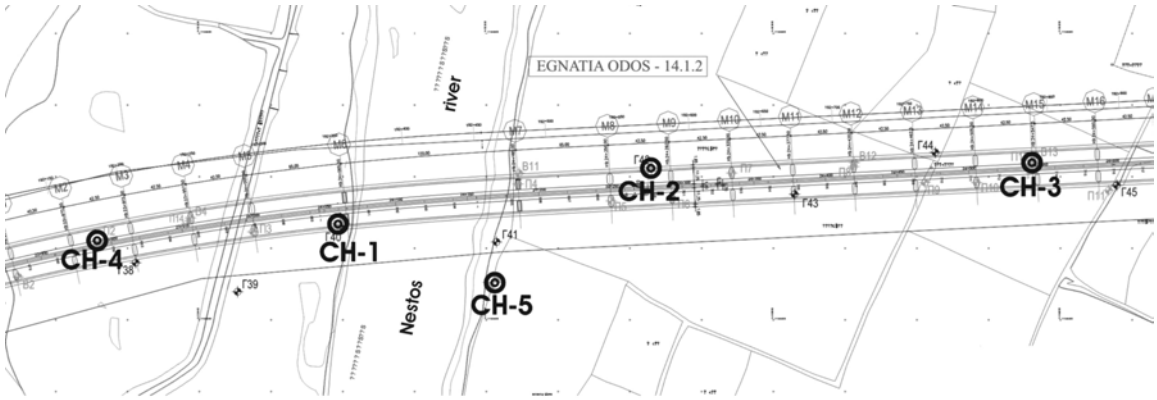

Figure 2: Topography map of the study area showing the location of the wells, presented with black circles. A total number of 12 boreholes were used for the experiment.

propagating shear waves (SV). The radial component senses the propagating compression waves (P) and the tangential component senses the horizontally propagating shear waves (SH). The hammer input and the receiver outputs are recorded by a Geometrics seismograph (StrataView-24bit, 24 channels). At the same time, the one of the geophones was also used to acquire DHS data set, when compression and shear waves are generated in the surface by the use of a sledgehammer with a triggering system. The source and receivers were moved to the next measurement depth and the process is continued until all desired measurements were taken.

We have used the SAC freeware interactive software (Seismic Analysis Code, developed by Lawrence Livermore Laboratory, University of California, 11/6/2000, Version 00.59.2) to pick arrivals times. Picking of P arrivals is much easier than S-arrival identification since it is always the first wave usually sharply arriving at the geophone.

For the S-waves, the picking of the onset of shear-wave motion in the presence of source generated noise (later cycles of P-motion or tube waves) can sometimes be challenging. Two methods of identification were applied: a) The conventional method of overlapping waveforms (from the "positive" and "negative" source polarity records) for each of the two geophones (usually vertical and a horizontal) is often adequate to obtain a crossover onset of shear-wave energy, as shown in Figure 3 and, b) alternatively we used the change of polarization direction of the wave field using particle motion diagrams. In practice for the P-wave arrival a linear particle motion along the direction of propagation is observed, whereas the S-wave arrival is associated with particle motion perpendicular to the direction of propagation. Using this method we could distinguish the component which "received" the S-wave motion by plotting component pairs, as is shown in Figure 4, since the orientation of the horizontal components of the recording geophones was unknown.

2.1 Preliminary data interpretation

When one receiver borehole is used, the travel time from source to the receiver is measured. This is referred to as direct travel time measurements. In the case that two receiver boreholes are used, the travel time between the receivers is measured, usually referred to as interval travel time measurements. Note that interval travel times are normally more accurate than direct travel times, since this method reduces timing errors caused by differences in seismic triggering, variations in source impulse characteristics and errors arising from variations in borehole size or mud-cake thickness near the transmitters. The wave velocities for compression and shear waves at a specific depth are easily determined by dividing the travel distances by the measured travel time. The travel distances were measured in the surface at the begging of the survey, assuming that the boreholes were vertical.

2.2 Tomographic interpretation of the Data

We used an iterative, 3-D tomographic inversion routine to determine the velocity structure betweens the wells and the ground (Soupios et al., 2001). The forward routine calculates the first arriving travel time using the revisited ray bending method, supplemented by an approximation of the first Fresnel zone at each point of

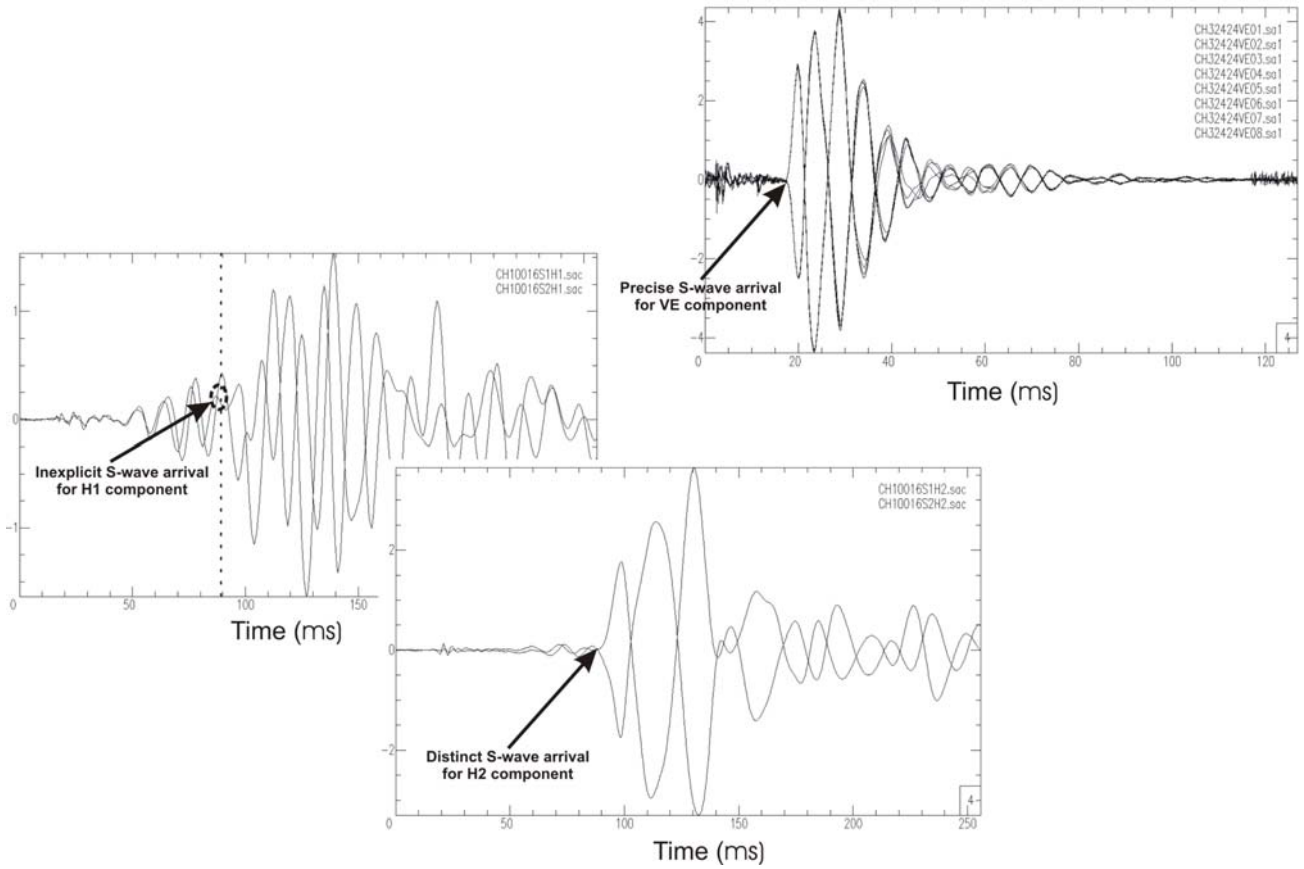

Figure 3: Detection of S-waves arrival using the conventional method of overlapping waveforms as recorded from horizontals and vertical component. It is obviously that the vertical component, receive the S-wave energy better than the horizontal components.

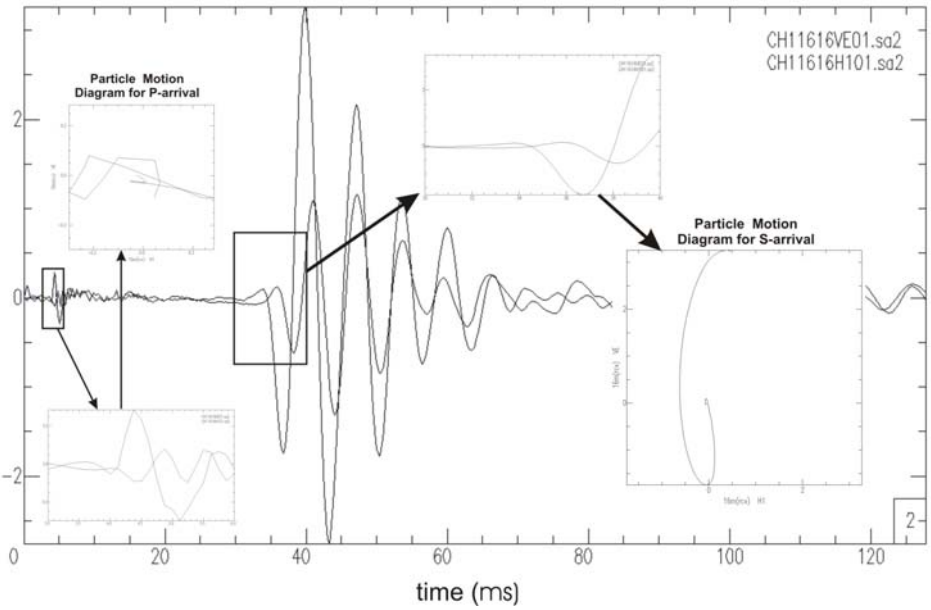

Figure 4: Picking of P and S-waves arrival applying the particle motion diagrams.

the ray, hence using physical and not only the mathematical rays (Fig. 5). Therefore, the algorithm computes the raypath, solves for the slowness using either an LSQR routine (Paige and Saunders, 1982) or an SVD algorithm and updates the model. The program iterates until the root-mean-square travel time residual cannot be further minimized.

We used a grid spacing of 2 meters in depth, similar to the source and receiver spacing during

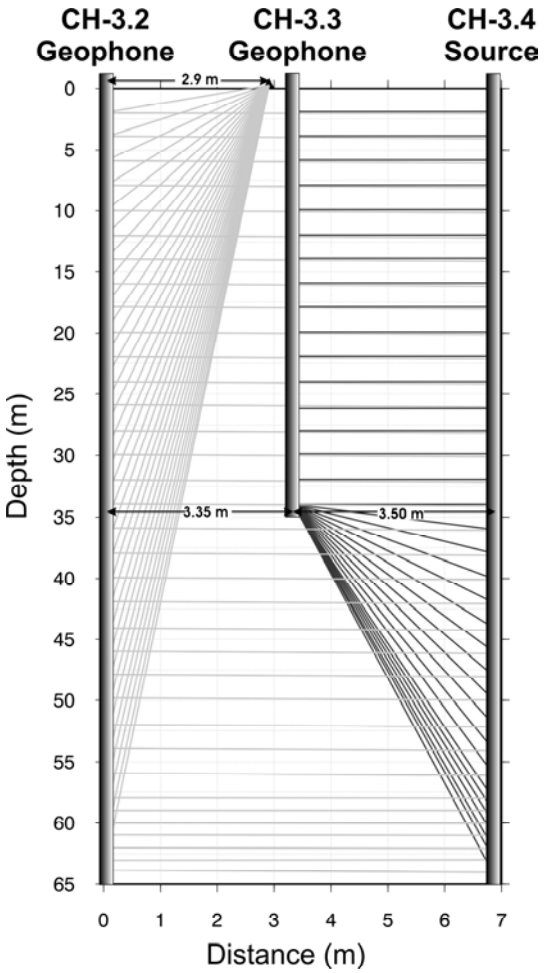

Figure 5: Ray coverage for the boreholes configuration in CH3 location.

data acquisition. The final velocity images (e.g. Fig. 6) are obtained performing a constrained least squares inversion scheme.

2.3 Estimation of the attenuation model

The attenuation model was estimated using the spectral ratio method as suggested by Neep et al. (1996). Specifically, the Q factor was calculated from the fit of a straight line to the spectral ratio of receiver and source power spectra recorded at different offset from the source.

The main assumptions of our approach are that: a) the receivers lie along a common raypath from the source and, b) the two power spectra can be linearly related by a simple attenuator operator. It is often necessary to apply windowing to the first few circles of the shear wave arrival before transform waveforms to the frequency domain in order to avoid contamination from lower velocity arrivals.

In this work, we have overlapped waveforms with different polarity and stacked “up” and

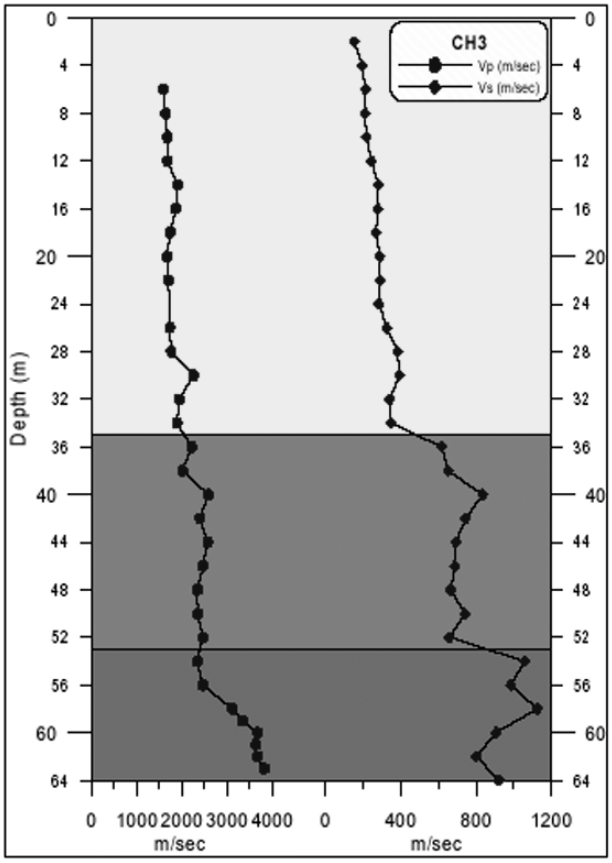

Figure 6: 1D velocity model for CH3 and its correlation with geological formations identified from the borehole.

“down” records to increase the signal-to-noise ratio before processing. Furthermore, we selected various time windows, keeping always the time of shear wave arrival as the lower limit of the window gate. Figure 7A shows the various windows (T1-T2, T1-T3, etc.) tested for the near offset geophone in both “up” and “down” waveforms, as they were recorded from the vertical component (SV waves) for borehole CH3 at the depth of 10m, while the corresponding spectra for the near- and far-offset geophones are presented in Figure 7B. It should be noted that the Q-estimates were practically stable for all time windows, as long as the main pulse of the S-waveform (window T1-T2 in Fig. 7A) was used.

The spectral ratio of the two spectra is presented in Figure 8A, where a clear linear decrease is observed for frequencies between 150-450Hz. Since the shear velocity for each depth is known from the previous tomographic step, the Q estimation was performed by fitting a straight line to the slope of the spectral ratio in the frequency range of 150-470 Hz. Furthermore, in order to stabilize the estimation of the

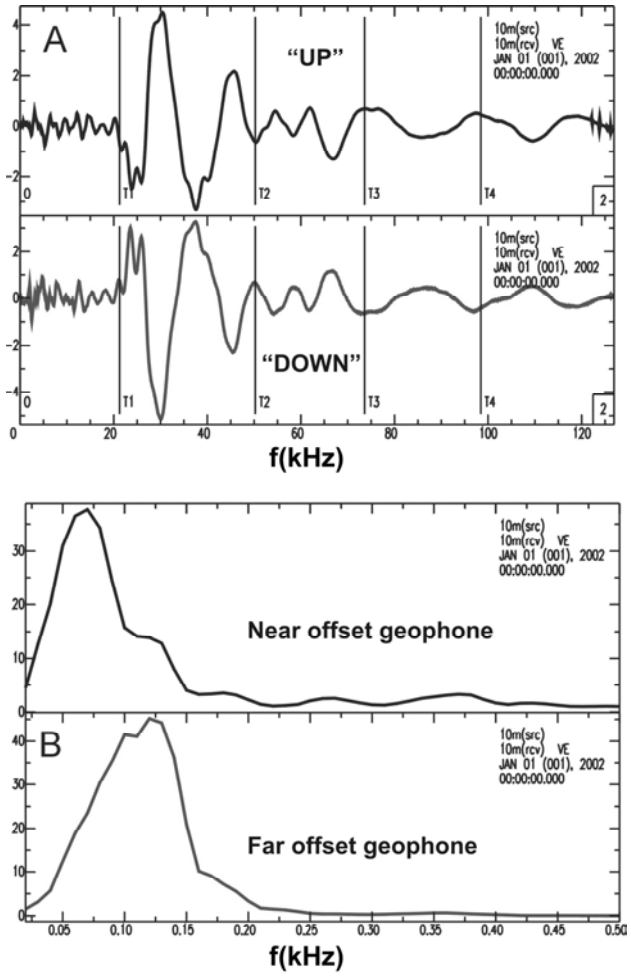

Figure 7: A) Time windows (T1-T2, T1-T3, etc.) selected for the S-wavetrains for the “up” and “down” source records tested for the Q-estimation. B) Spectra of the far- and near-offset geophones for borehole CH3 at the depth of 10m used for Q-estimation.

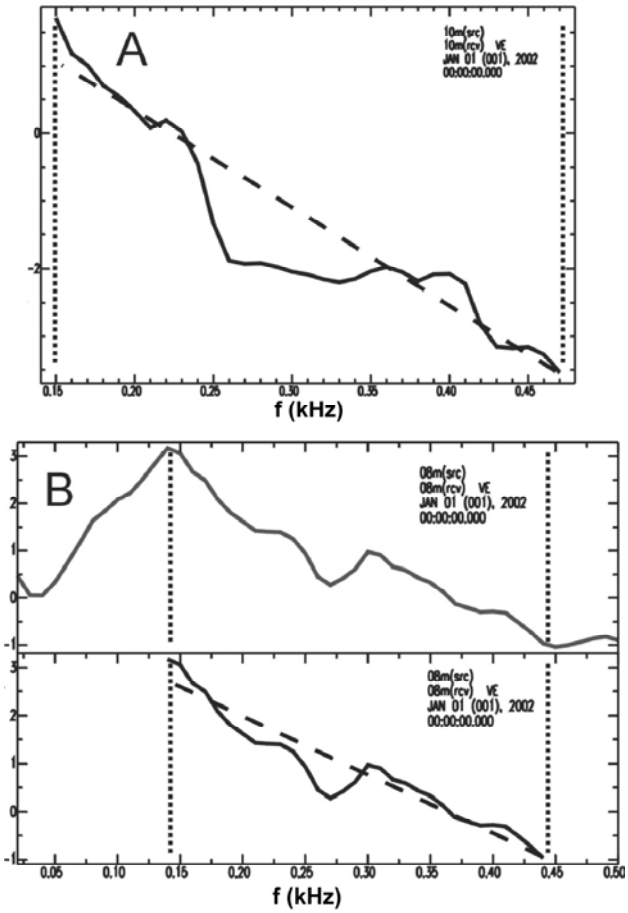

Figure 8: A) Linear decreasing logarithmic spectral ratio of the spectra presented in figure 7A. B) Average spectral ratio for the depth of 8 meters, as determined by the summation of spectral ratios for the depths of 4, 6, 8, 10 and 12 meters. The linearity of the spectral slope is more smooth and stable.

spectral slopes and improve the reliability of the attenuation results, we also estimated cumulative spectral ratios for overlapping depth intervals of 8 meters. The resulting spectral ratios are more stable and linear, as is shown in the example of Figure 8B where the average spectral ratio for the depth of 8 meters (5 cross-hole waveforms from the depths of 4-12 are used) when compared to Figure 8A.

Finally, for each borehole several additional elastic moduli (Poisson ratio, Young modulus and rigidity values) were also estimated at all depths for which data were available, in order to provide additional information to engineers for the calculation of the final dynamic response of the structure. A typical example of the finally obtained results for a selected borehole (CH1) is presented in the Table 1.

3. CONCLUSIONS

The use of engineering geophysics provided an efficient way to derive a geologic cross section (Fig. 9) to aid bridge engineers in their design of the Nestos bridge foundation.

The tomographic interpretation of the seismic data provides an explanation of the lateral variations in geology and allows the detailed description of not only elastic but also anelastic depth behavior, necessary for geotechnical site characterization.

The three-borehole approach allows not only the reliable estimation of attenuation parameters (Q-factor) but also the more reliable estimation of seismic velocities.

Table 1: Final Vp-Vs-Q_S model and variation of several elastic moduli such as Poisson ratio Young modulus and rigidity value for borehole CH-1, as well as Q (attenuation) values for several depths either individually estimated [Q(AV)] or from stacked spectral ratios [Q(AV-sm)] for different depth ranges.

CH-1									
Depth (m)	time (ms)	Vp (m/s)	time (ms)	Vs (m/s)	Poisson	Young (MPa)	Rigidity (MPa)	Q (AV)	Q (AV-sm)
2	4.7	638							
4	2.75	1028	43.5	157	0.488	196	66	12.0	
6	2.13	1276	43.25	158	0.492	199	67	24.4	
7									7.0
8	1.7	1533	41.75	164	0.494	214	71	18.3	
9									26.5
10	1.64	1577	38.5	177	0.494	251	84	34.4	
11									15.8
12	1.7	1533	36	190	0.492	287	96		
13									14.0
14	1.6	1608	35.5	192	0.493	295	99	13.2	
15									11.1
16	1.5	1691	34.2	200	0.493	318	106	5.2	
17									12.8
18	1.7	1533	35.5	192	0.492	295	99	10.4	
19									9.0
20	1.5	1691	28.5	240	0.490	457	153	8.2	
21									9.4
22	1.5	1691	30.8	222	0.491	392	131	8.4	
23									7.9
24	1.37	1812	23.4	292	0.487	676	227	10.5	
25									6.2
26	1.25	1941	22.04	310	0.487	763	256	5.0	
27									8.5
28	1.25	1941	20.7	330	0.485	863	291	5.2	
29									8.8
30	1.25	1941	20.7	330	0.485	863	291	95.2	
31									13.5

REFERENCES

ASTM D4228/D4228M –91, Standard Test Methods for Crosshole Seismic Testing, July 91, Committee D-18 on Soil and Rock.

Klimis, N.S., C.B. Papazachos and Ch.F. Efremidis, 1999. Determination of the behavior of a sedimentary rock mass: comparison of measured static and dynamic properties, Proc. of the 9th Int. Congress on Rock Mechanics, Paris, France, August 25-28, 1999.

Luna, R. and H. Jadi, 2000. Determination of dynamic soil properties using geophysical methods. Proceedings of the First International Conference on the Application of Geophysical and NDT Methodologies to Transportation Facilities and Infrastructure—Geophysics 2000. Federal Highway Administration, Saint Louis, MO. Paper No. 3 –1, 15 pp.

Neep, J.P., M.S. Sams, M.H. Worthington and K.A. O’Hara-Dhand, 1996. Measurement of seismic attenuation from high-resolution crosshole data, Geophysics, Vol. 61, No. 4, pp 1175-1188.

New, B.M., 1985. An example of tomographic and fourier microcomputer processing of seismic records, Quarterly Journal of Engineering Geology 18 (4): 335-344.

Paige, C.C. and M.A. Saunders, 1982. LSQR: An algorithm for sparse linear equations and sparse least squares, A.C.M. Trans. Math. Software, 8, 43-71.

Rechtien, R.D., 1996. In Situ Liquefaction Investigation

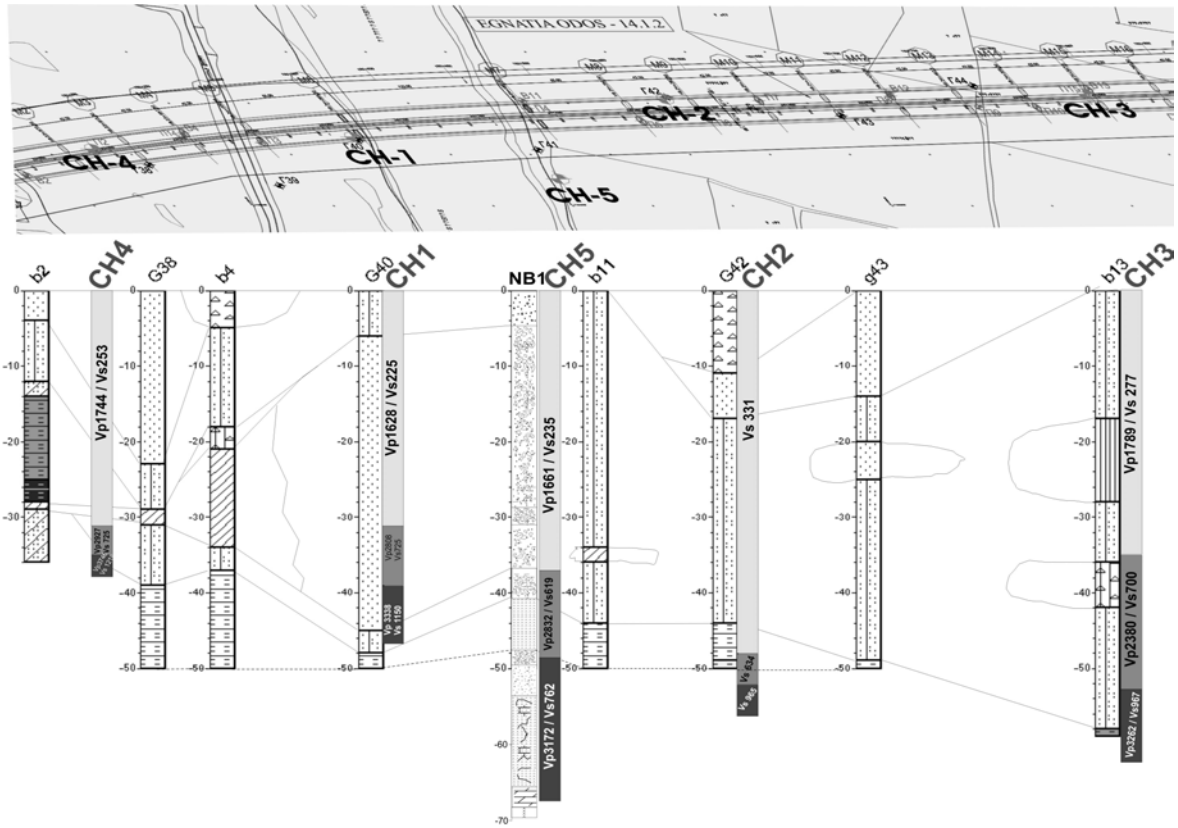

Figure 9: A cross section of the area from the combined interpretation of the borehole logs and geophysical measurements is obtained. Three stromatographic units are found, a) a formation with poorly–graded gravels, gravel-sand mixtures and little or no fines (Vp=1705m/s, Vs=254m/s), b) a weathered and fractured basement consist of gneiss (Vp=2737m/s, Vs=681m/s) and c) the rigid gneiss basement (Vp=3379m/s, Vs=1184m/s).

of Liquefaction Potential of Soils. Report GL-96-1-US Army Corps of Engineer, Waterways Experiment Station. 46 pp.

Sams, M. and D. Goldberg, 1990. The validity of Q estimates from borehole data using spectral ratios, Geophysics, 55, No. 1, pp 97-101.

Soupios, P.M., C.B. Papazachos, C. Juhlin and G.N. Tsokas, 2001. Non-linear three dimensional travel-time inversion of crosshole data with an application in the area of middle Urals, Geophysics, 66, 627-636.